A Hybrid Full-Wave Analysis of Via-Hole Grounds Using Finite-Difference and Finite-Element Time-Domain Methods

Dongsoo Koh, *Student Member, IEEE,* Hong-bae Lee, *Member, IEEE,* and Tatsuo Itoh, *Fellow, IEEE*

***Abstract*— A hybrid full-wave analysis using finite-difference time-domain (FDTD) and finite-element time-domain (FETD) methods is developed to analyze locally arbitrarily shaped microwave structures. This hybrid method employs the standard FDTD method with super-absorbing Mur's first-order absorbing-boundary condition (ABC) and the FETD method using the second-order vector prism elements. An interpolation scheme is proposed for communicating between the FDTD and FETD fields, which will not require the effort of fitting the FETD mesh to the FDTD cells in the interface region. This method is applied to calculate the scattering parameters of single and multiple cylindrical via holes in a microstrip structure. Applying FETD to the via-hole grounds and FDTD to the remaining region preserves the advantages of both FETD flexibility and FDTD efficiency. A comparison of the results with the mode-matching data and the FDTD staircasing data verifies the accuracy of the proposed method.**

***Index Terms*—Shape function, vector prism elements, via-hole grounds.**

I. Introduction

THE finite-difference time-domain (FDTD) method has a number of advantages in analyzing three-dimensional (3-D) microwave structures due to its simplicity and numerical efficiency [1], [2]. Making use of the uniform mesh in the conventional FDTD algorithm does not require any special mesh generation scheme and storage for the mesh. However, the use of box-shaped Cartesian coordinate uniform meshes in the conventional FDTD algorithm causes difficulties while dealing with curved structures and locally detailed structures. Typically, curved structures have been analyzed using the staircasing approximations [3], which requires finer meshes and dramatic increases in memory size as well as longer computational time caused by using the smaller time-step size to satisfy the Courant stability condition [4]. The same problems can be encountered in employing very fine meshes in the entire computational domain for the locally detailed structures.

Several methods have been developed to overcome these difficulties in the FDTD method. The nonorthogonal FDTD algorithm has been introduced to solve uniform and uncurved, but oblique structures [5], and later improved to analyze 3-D structures including curved shapes [6], [7]. Using covariant and contravariant components of $\vec{E}$ and $\vec{H}$ fields to obtain a finite-difference approximation of the integral forms of Maxwell's equations gives an important advantage in that the nonorthogonal FDTD algorithm can have the same form as the conventional FDTD algorithm. However, this method still requires longer computational time and larger memory size. The discrete surface integral (DSI) method has been also proposed to analyze general structures [8]. This method can be regarded as a generalization of the regular FDTD method since it reduces to the conventional FDTD method when structured orthogonal hexahedral grids are used. However, this method needs large memory size due to the requirement for the dual grid as well as the primary grid. A locally conformed FDTD algorithm has been studied for efficiently analyzing locally arbitrarily shaped structures [9]. This method performs the conventional FDTD leap-frog scheme and then corrects the field in order to take into account the metal structures which do not conform to the FDTD mesh by using the integral form of Maxwell's equations. Different geometries require different correction procedures, which can be a disadvantage of this method.

The finite-element time-domain (FETD) method has also been developed to improve flexibility in modeling structures by retaining the advantage of time-domain analysis [10]–[12]. Although this method can have no geometric limitations in modeling structures, it can be less efficient than the FDTD method because it requires the system of equations to be solved for each time step. Recently, a hybrid method incorporating the FETD method into the FDTD method was developed and applied to the electromagnetic scattering problem of two-dimensional (2-D) circular-shaped dielectric cylinders [13]. By conforming only the circular structures using FETD while applying FDTD elsewhere, a tradeoff between the FETD flexibility and the FDTD numerical efficiency can be obtained. However, the FDTD and FETD mesh-matching method in the interface region can contribute difficulty in the mesh generation of the FETD region.

This paper proposes a new FDTD and FETD hybrid method by introducing an interpolation scheme for communicating between the FDTD field and the FETD field in the interface region. In this method, one can avoid the effort of fitting the FETD mesh to the FDTD cells in the interface. This hybrid method is applied to analyze single and multiple via-hole grounds in microstrip. This is a 3-D problem having both cylindrical and rectangular boundaries, as described in detail later.

Manuscript received March 31, 1997; revised August 10, 1997.

The authors are with the Electrical Engineering Department, University of California at Los Angeles, Los Angeles, CA 90095 USA.

Publisher Item Identifier S 0018-9480(97)08341-5.

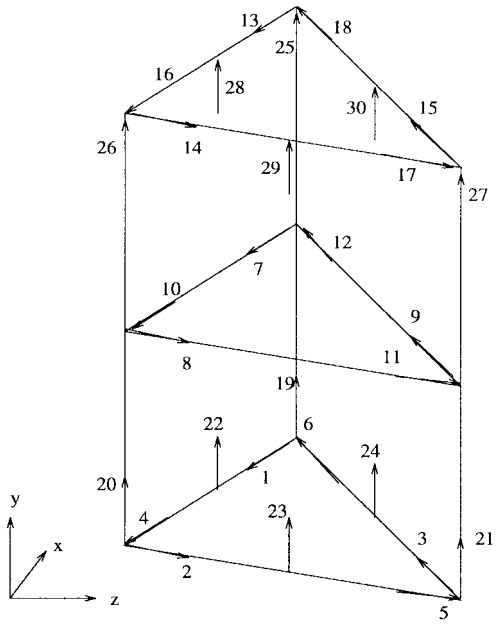

Fig. 1. The prism element.

Applying the FETD to the part of the FDTD region including via-hole grounds and the FDTD elsewhere preserves the advantages of both FDTD and FETD. In addition, changing the structure inside the FETD region does not require any change in the FDTD parameters, which can be a great advantage in design sensitivity analysis because different structures can be analyzed by changing only the FETD meshes. The comparison between the scattering parameter results obtained with the proposed hybrid method, mode-matching data [14], and FDTD staircasing data verifies the accuracy of this analysis.

II. Hybrid-Analysis Technique Using FDTD and FETD

The hybrid analysis proposed here employs the standard FDTD method with super-absorbing Mur's first-order absorbing-boundary condition (ABC) [15] and the FETD method using the second-order vector prism element [16], [17].

A. FETD Formulation

Starting from the source-free Maxwell's two-curl equations in a linear isotropic region, the vector-wave equation can be obtained as

$$\nabla \times \nabla \times \vec{E} + \mu\epsilon \frac{\partial^2 \vec{E}}{\partial t^2} = 0. \tag{1}$$

Applying the weak form formulation or the Galerkin's procedure to (1) gives

$$\int (\nabla \times \vec{E}) \cdot (\nabla \times \vec{W})\, dv + \int \mu\epsilon \vec{W} \cdot \frac{\partial^2 \vec{E}}{\partial t^2}\, dv = \int \vec{W} \cdot (\nabla \times \vec{E} \times \hat{n})\, ds \tag{2}$$

where $\vec{W}$ is the weighting function defined using the second-order vector prism element [16], [17].

The prism element is composed of 30 edge elements, as shown in Fig. 1. With the shape function, the electric field inside the prism element can be interpolated as

$$\begin{aligned}\vec{E}(r,t) = \sum_{l=1}^{3} \Bigg[&\sum_{i=1}^{3} L_i \frac{l_i}{\Delta} (b_j \hat{z} + c_j \hat{x})\, f_{yl} \mathcal{E}_{te}(t)_{i+6(l-1)} \\ &- \sum_{i=1}^{3} L_j \frac{l_i}{\Delta} (b_i \hat{z} + c_i \hat{x})\, f_{yl} \mathcal{E}_{te}(t)_{i+3+6(l-1)} \Bigg] \\ + \sum_{l=4}^{5} \Bigg[&\sum_{i=1}^{3} L_i (2L_i - 1)\, f_{yl} \mathcal{E}_{ye}(t)_{i+6(l-1)} \\ &+ \sum_{i=1}^{3} 4 L_i L_j f_{yl} \mathcal{E}_{ye}(t)_{i+3+6(l-1)} \Bigg] \hat{y}\end{aligned} \tag{3}$$

where

$$\begin{aligned}\mathcal{E}_{te}(t)_k &= \vec{E}(r,t) \cdot \hat{t}_k, \qquad k = 1, 2, \cdots, 18 \\ \mathcal{E}_{ye}(t)_k &= \vec{E}(r,t) \cdot \hat{y}_k, \qquad k = 19, 20, \cdots, 30\end{aligned} \tag{4}$$

and

$$\begin{aligned}f_{y1} &= L_{y1}(2L_{y1} - 1) \\ f_{y2} &= 4L_{y1}L_{y2} \\ f_{y3} &= L_{y2}(2L_{y2} - 1) \\ f_{y4} &= L_{y1} \\ f_{y5} &= L_{y2}.\end{aligned} \tag{5}$$

In (4), $\hat{t}_k$ and $\hat{y}_k$ are the unit vector of the kth edge in the prism element (Fig. 1). Therefore, $\mathcal{E}_{te}(t)_k$ and $\mathcal{E}_{ye}(t)_k$ represent the state variables of the kth edge in FETD, which can also be interpreted as electric fields. In (3) and (5), L_i's are the barycentric coordinates of a triangle, and L_{yi}'s are the first-order Lagrange interpolation polynomials between upper and lower triangular faces, which are expressed as [16], [17]

$$L_i = \frac{a_i + b_i z + c_i x}{2\Delta} \tag{6}$$

and

$$\begin{aligned}L_{y1} &= \frac{y_u - y}{2l_y} \\ L_{y2} &= \frac{y - y_l}{2l_y}.\end{aligned} \tag{7}$$

The variables y_u and y_l in (7) are the y-coordinates of the upper triangle and the lower triangle in the prism element and $2l_y$ corresponds to the difference between y_u and y_l.

In the finite differencing of (2) in time, the unconditionally stable backward difference is used [12], which gives

$$\begin{aligned}\sum_{e=1}^{N^e} &([K^e][E^e]^n \\ &= [F_s^e][E^e]^n + 2[F_v^e][E^e]^{n-1} - [F_v^e][E^e]^{n-2}\big)\end{aligned} \tag{8}$$

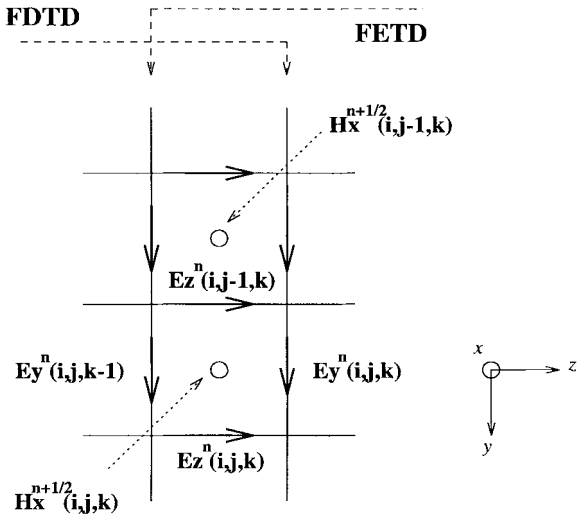

Fig. 2. The FDTD and FETD interface region.

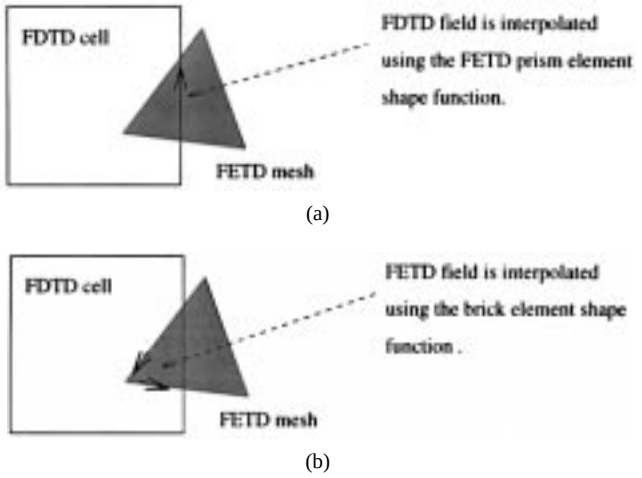

Fig. 3. Interpolation scheme for communicating between FDTD and FETD fields at the interface. (a) FETD → FDTD. (b) FDTD → FETD.

where

$$K_{ij}^e = \int_v (\nabla \times \vec{W}_i^e) \cdot (\nabla \times \vec{W}_j^e)\, dv + \frac{\mu\epsilon^e}{\delta t^2} \int_v \vec{W}_i^e \cdot \vec{W}_j^e\, dv$$
$$F_s^e = \int_s \vec{W}_i^e \cdot (\nabla \times \vec{W}_j^e \times \hat{n})\, ds$$
$$F_v^e = \frac{\mu\epsilon^e}{\delta t^2} \int_v \vec{W}_i^e \cdot \vec{W}_j^e\, dv \tag{9}$$

N^e is the number of the total edge elements and $[E^e]^n$ represents the state variable vector at the time-step n.

B. Hybridizing the FDTD and FETD Analyses

The right-hand side (RHS) of (8) (the load vector of the FETD) shows the necessity of knowing the electric-field values for two previous time steps, as well as the boundary values at the present time step. The boundary values calculated from FDTD become the Dirichlet boundary conditions on the FETD boundary, and are used to solve the inner field of the FETD region. The FETD region is chosen to be a brick replacing the part of the FDTD region and includes the locally arbitrarily shaped structures. This choice of FETD region provides a great advantage when different arbitrarily shaped structures need to be analyzed, because only the FETD mesh change will be required without affecting the FDTD variables.

Fig. 2 shows the FDTD and FETD interface region in a 2-D view. One cell size of FDTD region is to be overlapped in the FETD region. In the FDTD time-marching procedure $Ey^n(i, j, k-1)$, $Ez^n(i, j, k)$, and $Ez^n(i, j-1, k)$ are updated, but the FDTD boundary value $Ey^n(i, j, k)$ cannot be updated because $Hx^{n-(1/2)}(i, j, k+1)$ does not exist. The updated interface values are employed in the FETD through the surface integrals of (9) to calculate the inner field in the FETD domain. The calculated inner field is used to update the FDTD boundary value, $Ey^n(i, j, k)$. Once $Ey^n(i, j, k)$ is updated, the $Hx^{n+(1/2)}(i, j, k)$ can be calculated from the H-field updating procedure of FDTD. This completes one time-marching procedure of the hybrid method.

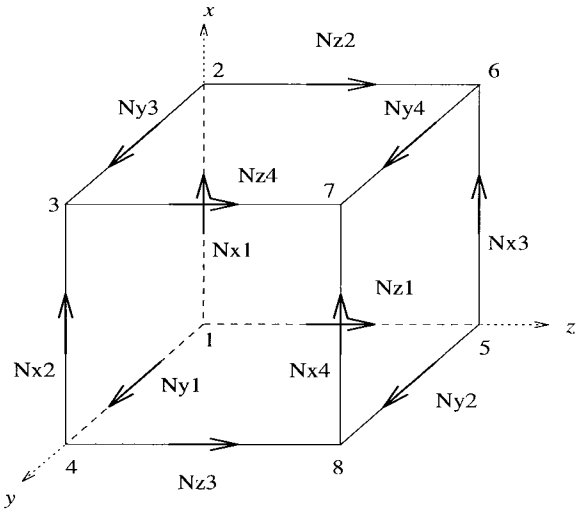

Fig. 4. The regular brick element.

This hybrid method makes use of an interpolation scheme in communicating between the FETD and FDTD fields at the interface. Fig. 3 explains this communication method. After the FETD calculation, the FDTD interface field is interpolated using the FETD prism element shape function (3). On the other hand, the FETD interface field can be interpolated using the regular brick element shape function with the FDTD interface field. Fig. 4 shows the regular brick element [18]. By substituting the FDTD interface field to the edge elements of the regular brick element, the electric field inside the cell can be interpolated as

$$\vec{E}(r, t) = \hat{x} \sum_{i=1}^{4} N_{xi}^e E_{xi}^e + \hat{y} \sum_{i=1}^{4} N_{yi}^e E_{yi}^e + \hat{z} \sum_{i=1}^{4} N_{zi}^e E_{zi}^e \tag{10}$$

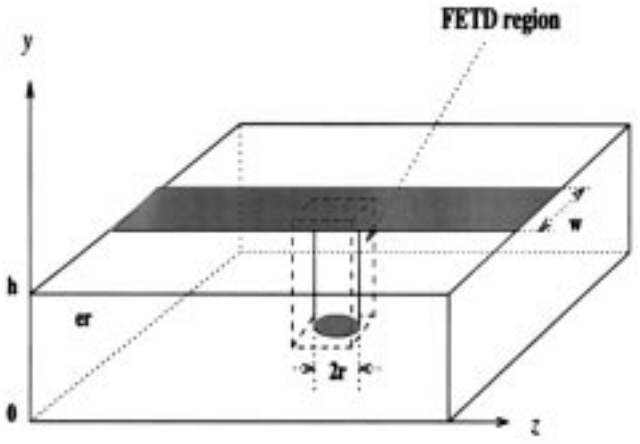

Fig. 5. The via-hole grounded microstrip.

where N_{xi}^e's are defined as

$$N_{x1}^e = \frac{(y_u - y)(z_u - z)}{l_y^e l_z^e}$$

$$N_{x2}^e = \frac{(y - y_l)(z_u - z)}{l_y^e l_z^e}$$

$$N_{x3}^e = \frac{(y_u - y)(z - z_l)}{l_y^e l_z^e}$$

$$N_{x4}^e = \frac{(y - y_l)(z - z_l)}{l_y^e l_z^e}. \tag{11}$$

N_{yi}^e and N_{zi}^e can be derived from (11) using the cyclical relationships of x, y, z. The l_x^e, l_y^e, and l_z^e correspond to the Δx, Δy, and Δz of the FDTD cell. Now, the FETD interface field can be easily calculated using (4). This scheme is more general than the FDTD and FETD mesh-matching method [13] because the mesh-matching effort is avoided.

III. Numerical Results

This hybrid method was applied to characterize the cylindrical via-hole grounds in microstrip. The via-hole region is replaced by the FETD region, as shown in Fig. 5. Since the microstrip and ground plane coincide with the top and the bottom boundaries of the FETD region, the Dirichlet boundary conditions are applied to the top and the bottom as well as the via-hole cylinder wall. This reduces the matrix size in the FETD analysis and increases the computational efficiency.

The parameters of the first analyzed via-hole grounded microstrip structure are as follows: via-hole diameter is 0.6 mm, microstrip width is 2.3 mm, and substrate thickness is 0.794 mm. Lastly, the substrate has a low dielectric constant ($\epsilon_r = 2.32$). Fig. 6(a) shows the cross-sectional view of the FETD mesh for the 0.6-mm diameter via hole, which was employed in the hybrid method. For the good quality triangular meshes, the Delaunay tessellation algorithm was used. The same structure was also simulated using the FDTD staircasing approximations. Fig. 7 depicts the cross section of the FDTD staircasing model of the via hole. In order to get the resolution in Fig. 7, the 2.3-mm-wide microstrip was divided into 40 cells. In the hybrid method, only six cells were used for the microstrip in the FDTD region and

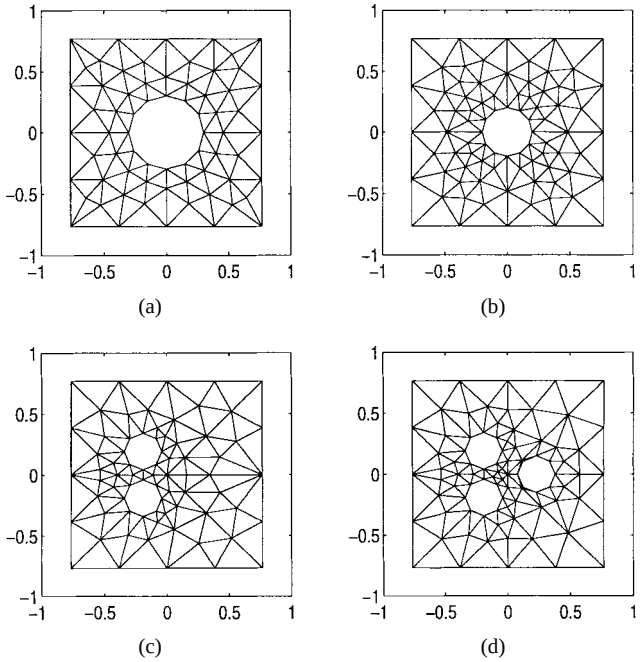

Fig. 6. FETD meshes for the via holes. (a) $2r = 0.6$ mm, (b) $2r = 0.4$ mm, (c) $2r = 0.3$ mm, and (d) $2r = 0.3$ mm.

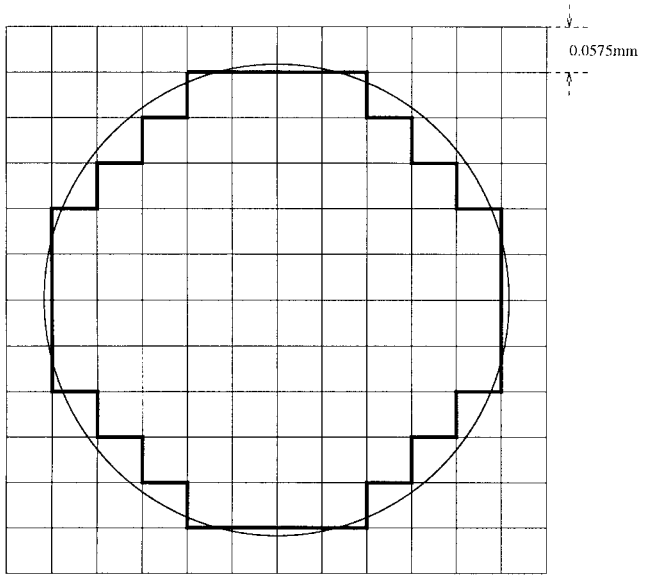

Fig. 7. FDTD staircasing model for the 0.6-mm diameter via hole.

$4 \times 3 \times 4$ FDTD cells were replaced by the FETD region among the total $60 \times 20 \times 100$ FDTD cells. Fig. 8 compares the $|S_{21}|$'s of this via-hole grounded microstrip calculated by this hybrid method, the mode-matching method [14], and the FDTD staircasing approximations. A very good agreement was observed between the hybrid method data and the mode-matching data. In the next step, the via-hole grounds with 0.4-mm diameter [as shown in Fig. 6(b)] were analyzed, and the result is shown in Fig. 9. The hybrid method gives a good prediction of $|S_{21}|$ for various via-hole diameters.

Practically, the ground effect of a large diameter via hole can be obtained using multiple small diameter via holes. To begin with, the two via-hole problem was chosen, as shown in Fig. 6(c). Both via holes have the same diameter ($2r = 0.3$

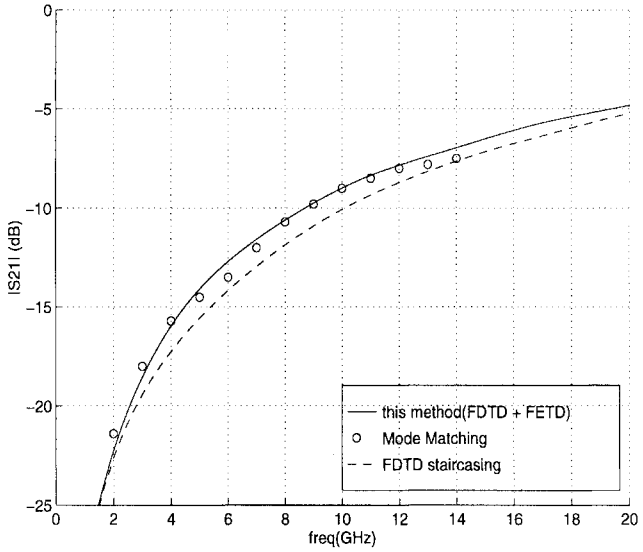

Fig. 8. $|S_{21}|$ of the via-hole grounded microstrip ($\epsilon_r = 2.32$, $w = 2.3$ mm, $h = 0.794$ mm, $2r = 0.6$ mm).

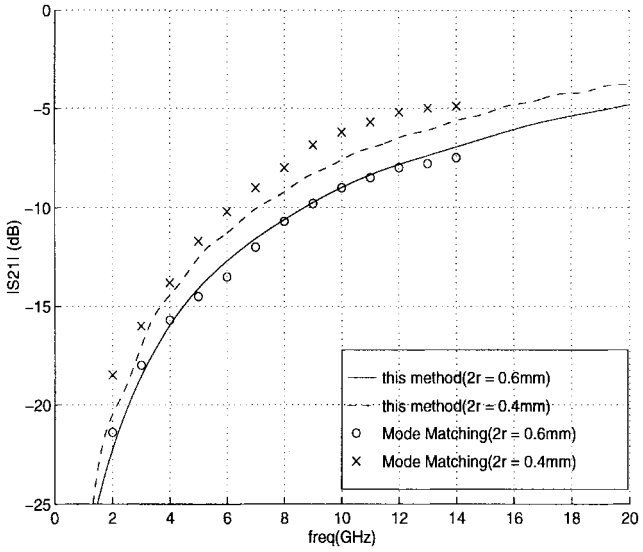

Fig. 9. $|S_{21}|$ of the via-hole grounded microstrip ($\epsilon_r = 2.32$, $w = 2.3$ mm, $h = 0.794$ mm).

mm). For reference, the two via-hole grounds with the square via holes ($a = b = 0.3$ mm) were also analyzed using only the FDTD method. Fig. 10 shows the square via holes in the FDTD cells. The $|S_{21}|$'s of these via-hole grounds are shown in Fig. 11. The result of the via-hole grounded microstrip with two circular via holes is very close to that of the via-hole grounded microstrip with one circular via hole having larger diameter size ($2r = 0.6$ mm). The via-hole grounded microstrip with two square via holes shows lower $|S_{21}|$ than one with circular ones (Fig. 11). This result is shown to be reasonable because the effective via-hole area of the square via holes is larger than the circular via holes. In the next step, three via holes were analyzed for the grounded microstrip. Fig. 6(d) shows the cross-sectional view of the three via-hole grounds. $|S_{21}|$ of the three via-hole grounds is at least 3 dB less than $|S_{21}|$ of the two via-hole grounds over a wide frequency band (Fig. 12).

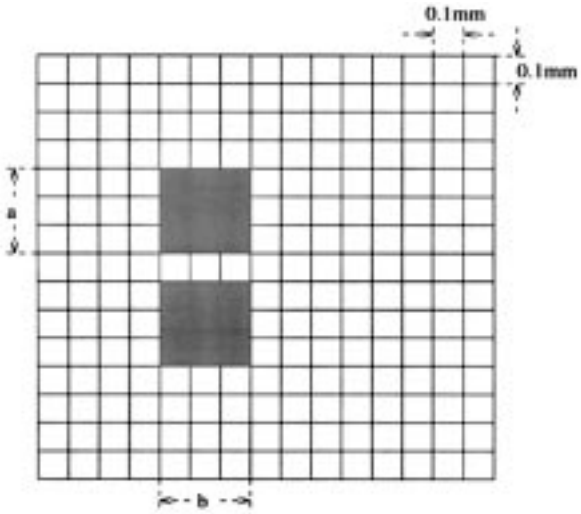

Fig. 10. The FDTD modeling for the two via holes ($\epsilon_r = 2.32$, $w = 2.3$ mm, $h = 0.794$ mm, $a = b = 0.3$ mm).

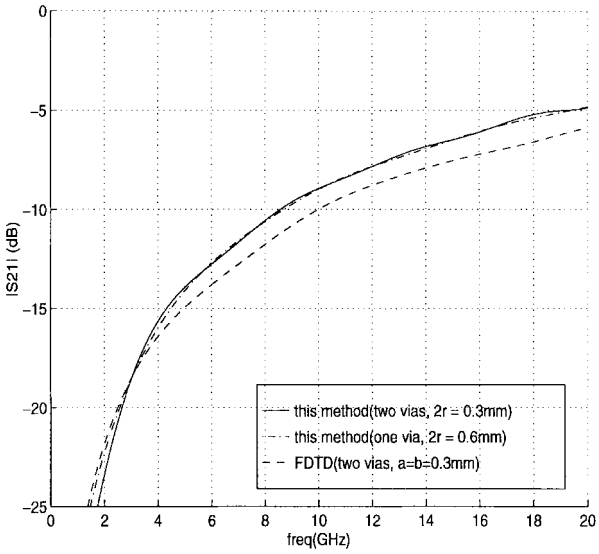

Fig. 11. $|S_{21}|$ of the grounded microstrip with two via holes ($\epsilon_r = 2.32$, $w = 2.3$ mm, $h = 0.794$ mm).

At this moment, it is worthwhile to mention that only the FETD meshes were changed for analyzing four different via-hole grounds without affecting the FDTD variables. In Fig. 6, one can notice that the outer boundaries of all the FETD meshes are fixed and correspond to 4×4 FDTD cells. For staircasing approximations, the cell size and the Δt size need to be changed for different structures. Therefore, the hybrid method is more suitable for investigating the design sensitivity of locally arbitrarily shaped structures. For example, one can analyze circuit performance according to the variations of the design parameters, such as structure geometries.

This hybrid method makes use of the quasi-minimal residue (QMR) iterative method [19] to solve the system of equations in FETD for each time step. Solving the system of equations for every time step can be inefficient. However, the FETD region in this hybrid method occupies only a small part of the entire domain and the overall computational efficiency is not affected. For example, the number of edge elements for the

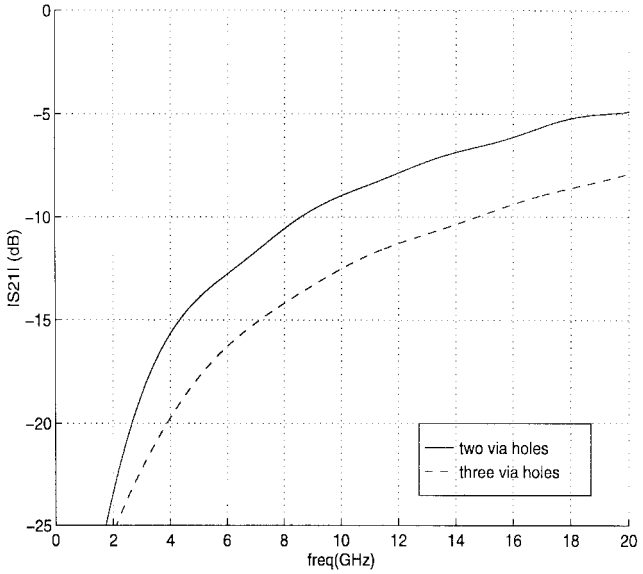

Fig. 12. $|S_{21}|$ of the via-hole grounded microstrip ($\epsilon_r = 2.32$, $w = 2.3$ mm, $h = 0.794$ mm).

0.6-mm diameter via-hole ground is 448. The hybrid method requires 23 Mb and takes 8.1 s for one time step running on a Sun SPARC station 20. In the meantime, the FDTD staircasing approximations (Fig. 7) using a total of $140 \times 40 \times 180$ cells require 54 Mb and takes 7.2 s for one time step running in the same machine. Since the Δt size of the FDTD staircasing approximations is chosen to be 2.5 times less than the Δt size of the hybrid method ($\Delta t = 0.25 \times 10^{-12}$ s), the computational time of the FDTD staircasing is at least two times longer than that of the hybrid method.

IV. Conclusion

A hybrid full-wave analysis using FDTD and FETD methods has been introduced and applied to successfully characterize via-hole grounded microstrips. This method incorporates the conventional FDTD method using the super-absorbing Mur's first-order ABC and the FETD method having the second-order vector prism element as the shape function. The interpolation scheme for communicating between the FDTD and FETD fields at the interface, which is proposed in this analysis, does not require the effort of fitting the FETD mesh to the FDTD cells at the interface region. Four different via-hole ground structures have been analyzed by changing only the FETD mesh without affecting the FDTD parameters. This can be a great advantage for design sensitivity analysis of locally arbitrarily shaped structures. The required memory size and the computational time of the hybrid method have also been compared with those of the staircasing method, which shows the efficiency of the hybrid method. The accuracy of the hybrid method is verified using the mode-matching method and the FDTD staircasing approximations. This hybrid method can be applied toward analyzing 3-D locally arbitrarily shaped structures accurately and efficiently.

References

[1] X. Zhang and K. K. Mei, "Time-domain finite difference approach to the calculation of the frequency-dependent characteristics of microstrip discontinuities," *IEEE Trans. Microwave Theory Tech.*, vol. 36, pp. 1775–1787, Dec. 1988.

[2] D. M. Sheen, S. M. Ali, M. D. Abouzahra, and J. A. Kong, "Application of the three-dimensional finite-difference time-domain method to the analysis of planar microstrip circuits," *IEEE Trans. Microwave Theory Tech.*, vol. 38, pp. 849–857, July 1990.

[3] A. C. Cangellaris and D. B. Wright, "Analysis of the numerical error caused by the stair-stepped approximation of a conducting boundary in FDTD simulations of electromagnetic phenomena," *IEEE Trans. Antennas Propagat.*, vol. 39, pp. 1518–1525, Oct. 1991.

[4] A. Taflove and M. E. Brodwin, "Numerical solution of steady-state electromagnetic scattering problems using the time-dependent Maxwell's equations," *IEEE Trans. Microwave Theory Tech.*, vol. MTT-23, pp. 623–630, Aug. 1975.

[5] R. Holland, "Finite-difference solution of Maxwell's equations in generalized nonorthogonal coordinates," *IEEE Trans. Nucl. Sci.*, vol. NS-30, pp. 4589–4591, Dec. 1983.

[6] M. A. Fusco, M. V. Smith, and L. W. Gordon, "A three-dimensional FDTD algorithm in curvilinear coordinates," *IEEE Trans. Antennas Propagat.*, vol. 39, pp. 1463–1471, Oct. 1991.

[7] J.-F. Lee, R. Palandech, and R. Mittra, "Modeling three-dimensional discontinuities in waveguides using nonorthogonal FDTD algorithm," *IEEE Trans. Microwave Theory Tech.*, vol. 40, pp. 346–352, Feb. 1992.

[8] N. Madsen, "Divergence preserving discrete surface integral methods for Maxwell's equations using nonorthogonal unstructured grids," *J. Comput. Phys.*, vol. 119, pp. 34–45, June 1995.

[9] J. Fang and J. Ren, "A locally conformed finite-difference time-domain algorithm of modeling arbitrary shape planar metal strips," *IEEE Trans. Microwave Theory Tech.*, vol. 41, pp. 830–838, May 1993.

[10] J.-F. Lee, "WETD—A finite-element time-domain approach for solving Maxwell's equations," *IEEE Microwave Guided Wave Lett.*, vol. 4, pp. 11–13, Jan. 1994.

[11] J.-F. Lee and Z. Sacks, "Whitney elements time domain (WETD) methods," *IEEE Trans. Magn.*, vol. 31, pp. 1325–1329, May 1995.

[12] Z. S. Sacks and J.-F. Lee, "A finite-element time-domain method using prism elements for microwave cavities," *IEEE Trans. Electromag. Compat.*, vol. 37, pp. 519–527, Nov. 1995.

[13] R.-B. Wu and T. Itoh, "Hybridizing FD-TD analysis with unconditionally stable FEM for objects of curved boundary," in *IEEE MTT-S Dig*, Orlando, FL, May 1995, pp. 833–836.

[14] R. Sorrentino, F. Alessandri, M. Mongiardo, G. Avitabile, and L. Roselli, "Full-wave modeling of via hole grounds in microstrip by three-dimensional mode matching technique," *IEEE Trans. Microwave Theory Tech.*, vol. 40, pp. 2228–2234, Dec. 1992.

[15] K. K. Mei and J. Fang, "Superabsorption—A method to improve absorbing boundary conditions," *IEEE Trans. Antennas Propagat.*, vol. 40, pp. 1001–1010, Sept. 1992.

[16] M. Koshiba, S. Maruyama, and K. Hirayama, "A vector finite-element method with the high-order mixed-interpolation-type triangular elements for optical waveguiding problems," *J. Lightwave Tech.*, vol. 12, pp. 495–502, Mar. 1994.

[17] K. Hirayama, M. S. Alam, Y. Hayashi, and M. Koshiba, "Vector finite element method with mixed-interpolation-type triangular-prism element for waveguide discontinuities," *IEEE Trans. Microwave Theory Tech.*, vol. 42, pp. 2311–2316, Dec. 1994.

[18] J. Jin, *The Finite Element Method in Electromagnetics.* New York: Wiley, 1993.

[19] Y. Saad, *Iterative Methods for Sparse Linear Systems.* Boston, MA: PWS, 1996.

Dongsoo Koh (S'90) was born in Seoul, Korea, on February 24, 1967. He received the B.S. and M.S. degrees in electronic engineering from Sogang University, Seoul, Korea, in 1989 and 1991, respectively, and is currently working toward the Ph.D. degree in electrical engineering from the University of California at Los Angeles (UCLA).

From February 1993 to August 1993, he worked as a Research Engineer at Korea Telecom Research Center, Seoul, Korea. Since 1993, he has been a Graduate Student Researcher and a Teaching Assistant in the Electrical Engineering Department, UCLA. His research interests include the analysis and design of RF, microwave and millimeter-wave integrated circuits, and the development of full-wave electromagnetic simulation tools.

Hong-bae Lee (M'96) was born on August 11, 1966, in Seoul, Korea. He received the B.S., M.S., and Ph.D. degrees, all in electrical engineering, from Seoul National University, Seoul, Korea, in 1989, 1991, and 1995, respectively.

From March 1995 to February 1996, he was a Researcher of EESRI at Seoul National University. He is currently a Post-Doctoral Fellow in the Electrical Engineering Department, University of California at Los Angeles (UCLA). His current research interests include the numerical methods for microwave and millimeter-waves devices, optimum design based on the full-wave analysis, actuator design, and active circuit design with full-wave analysis.

Tatsuo Itoh (S'69–M'69–SM'74–F'82) received the Ph.D. degree in electrical engineering from the University of Illinois at Urbana, in 1969.

From September 1966 to April 1976, he was with the Electrical Engineering Department, University of Illinois at Urbana. From April 1976 to August 1977, he was a Senior Research Engineer in the Radio Physics Laboratory, SRI International, Menlo Park, CA. From August 1977 to June 1978, he was an Associate Professor at the University of Kentucky, Lexington. In July 1978, he joined the faculty at the University of Texas at Austin, where he became a Professor of electrical engineering in 1981, and Director of the Electrical Engineering Research Laboratory in 1984. During the summer of 1979, he was a Guest Researcher at AEG-Telefunken, Ulm, Germany. In September 1983, he was selected to hold the Hayden Head Centennial Professorship of Engineering at the University of Texas at Austin. In September 1984, he was appointed Associate Chairman for Research and Planning of the Electrical and Computer Engineering Department at the University of Texas at Austin. In January 1991, he joined the University of California at Los Angeles, as Professor of electrical engineering and Holder of the TRW endowed chair in microwave and millimeter-wave electronics. He is currently Director of the Joint Services Electronics Program (JSEP) and Director of Multidisciplinary University Research Initiative (MURI) Program at UCLA. He was an Honorary Visiting Professor at both Nanjin Institute of Technology, China, and at the Japan Defense Academy. In April 1994, he was appointed as Adjunct Research Officer for the Communications Research Laboratory, Ministry of Post and Telecommunication, Japan. He currently holds visiting professorships at the University of Leeds, Leeds, U.K., and is an External Examiner of the graduate program of City University of Hong Kong. He has authored or co-authored over 220 journal publications, 380 refereed conference presentations, and has authored over 20 books/book chapters in the area of microwaves, millimeter-waves, antennas, and numerical electromagnetics.

Dr. Itoh is a member of the Institute of Electronics and Communication Engineers (IEICE), Japan, Commissions B and D of USNC/URSI, and an honory life member of the Microwave Theory and Techniques Society. He served as the Editor of IEEE TRANSACTIONS ON MICROWAVE THEORY AND TECHNIQUES (1983–1985). He serves on the Administrative Committee of the IEEE Microwave Theory and Techniques Society. He was vice president (1989) and president (1990) of the Microwave Theory and Techniques Society. He was the Editor-in-Chief of IEEE MICROWAVE AND GUIDED WAVE LETTERS (1991–1994). He was the chairman of USNC/URSI Commission D (1988–1990), the vice chairman of Commission D of the International URSI (1991–1993) and chairman (1993–1996). He is on the Long Range Planning Committee of URSI, and serves on advisory boards and committees for a number of organizations including the National Research Council and the Institute of Mobile and Satellite Communication, Germany.